

# Preparation of semi-solid A356 Al-alloy slurry by introducing grain process

CHEN Zheng-zhou

Huili Machinery and Electric Co. Ltd., Cixi 315333, China

Received 7 June 2011; accepted 6 March 2012

**Abstract:** A preparation technology of semi-solid metal slurry introducing grain process (IGP) was developed. The effects of processing parameters on the microstructures of the semi-solid A356 Al-alloy slurries were investigated, and the formation mechanism and morphology controlling of the spherical primary  $\alpha(\text{Al})$  grains were discussed. The results show that when the preparing slurry is 4 kg, IG size is 10 mm, dosage is 3.5% and dumping temperature (DT) is 611–617 °C, the mean diameter of the primary  $\alpha(\text{Al})$  grains in the semi-solid slurries can reach 40–75  $\mu\text{m}$  and the shape factor can reach 0.82–0.89. When the IG size is 10 mm, DT is 613 °C and dosage is 2%–4%, the mean diameter can reach 45–82  $\mu\text{m}$  and the shape factors can reach 0.78–0.88. With decreasing DT or increasing dosage properly, the primary  $\alpha(\text{Al})$  grain morphology is better. When  $Q_R=Q_A$  and  $R_h=R_c$ , as long as the DT is suitable, excellent semi-solid slurry can be produced. As a result of the IG melting, a large amount of dendritic fragments can become the direct source of the primary  $\alpha(\text{Al})$  grains. Meanwhile, many undercooled areas are formed, where abundant primary  $\alpha(\text{Al})$  grains are multiplied by heterogeneous nucleation.

**Key words:** A356 Al alloy; semi-solid; introducing grain; primary  $\alpha(\text{Al})$

## 1 Introduction

Preparation of the semi-solid metal slurry with spherical primary phase is crucial in semi-solid rheofforming technology. At present, according to the formation or source of spherical primary phase, the existed preparation methods can be divided into two types generally. One is spherical primary phase which can self-produce in liquid alloy by various means, such as several stirring processes [1–3] and controlling nucleation methods [4–8]; the other is chemical grain refinement method [9–11], but this process changes the chemical composition of the semi-solid metal slurry. In addition, metal melt mixing process was put forward once [12–14], but the formation mechanism and morphology controlling of the spherical primary phase were not researched deeply.

The work presented introducing grain process (IGP) for preparing semi-solid meal slurry. The method is that the IGs are distributed evenly into the liquid alloy with a certain superheat, the chemical composition of which is the same with the preparing semi-solid slurry, and the microstructure of which belongs to traditional

solidification microstructure. After the IG is melted, the temperature of the liquid alloy is just near the liquidus temperature. The melted dendritic fragments become the direct source of primary  $\alpha(\text{Al})$  phase. From the test method, there are some similarities in mixed solid liquid casting process [15] and suspended casting method [16–18]. In the present work, using A356 Al alloy, the formation mechanism and morphology controlling of the spherical primary phase were investigated from the vision of the IG size, dosage and dumping temperature (DT).

## 2 Experimental

Commercial A356 Al alloy was used, its liquidus temperature and solidus temperature are 615 and 577 °C, respectively. The chemical composition of IG was the same with that of the commercial A356 Al alloy, in which primary  $\alpha(\text{Al})$  grains were dendrites, as shown in Fig. 1. The alloy was heated to 630 °C and then removed from a crucible resistance furnace, and the IGs were added evenly into the liquid alloy. When the liquid alloy was cooled to a set temperature, it was dumped to a collection crucible with dimensions of  $d127 \text{ mm} \times$

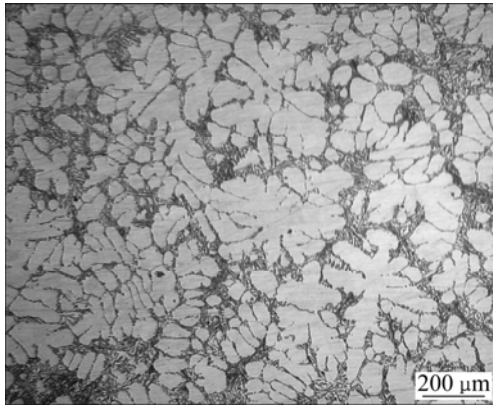


Fig. 1 OM image of IG

250 mm made of stainless steel. The temperature of the collection crucible was 300 °C. The schematic diagram of the preparation process is shown in Fig. 2. Each dose of slurry was approximately 4 kg. Two Ni–Cr/Ni–Si thermocouples were used to measure the temperatures of the liquid alloy and slurry, respectively, and the temperature displaying accuracy was  $\pm 1$  °C. To investigate the slurry microstructure, the collection crucible was cooled in cold water after dumping. The metallographic specimens were cut from the centre of the quenched slurries and then roughly ground, finely ground, polished and etched with 0.5% HF aqueous solution finally. A Neuphoto 21 optical microscope with quantitative metallography was utilized for the observation and quantitative measurement. The shape factor was calculated using  $F=4\pi A/P^2$ , where  $A$  and  $P$  represent the area and perimeter of the primary  $\alpha$ (Al) grain, respectively. Therefore,  $F$  is 1 for perfectly spherical grain.

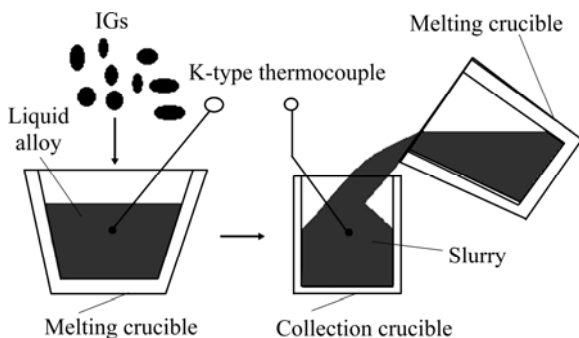


Fig. 2 Schematic of semi-solid A356 Al alloy slurry prepared by IGP

### 3 Results

#### 3.1 Effect of dosage on liquid alloy temperature

When the IG size is 10 mm, and the dosages are 2%, 3%, 3.5% and 4% (mass fraction), respectively, the cooling rates of the liquid alloy are shown in Fig.3.

Without IG, the cooling rate is 0.5 °C/s. However, with IG, the cooling process can be divided into two stages clearly. The first stage is rapid cooling stage, and the cooling rates are 2, 2.3, 2.6 and 3 °C/s, respectively. The second stage is slow cooling stage, and the cooling rates are 0.43, 0.44, 0.44 and 0.43 °C/s, respectively. There exists a transition temperature between the two cooling stages, which is 613–617 °C. Table 1 lists the characteristic data of the cooling curves in Fig. 3.

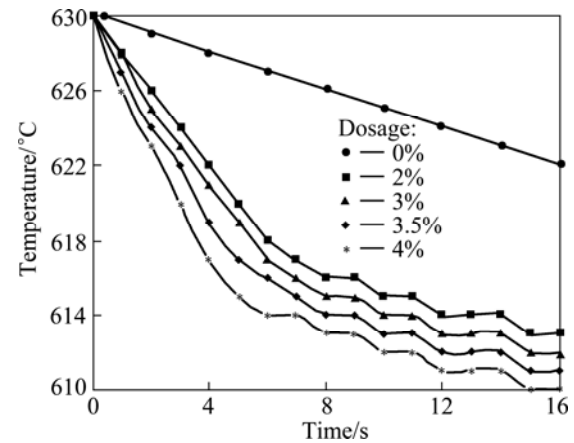


Fig. 3 Effect of IG dosage on liquid alloy temperature

Table 1 Characteristic data of cooling curves in Fig. 3

Dosage/%	First stage cooling rate/ (°C·s <sup>-1</sup> )	Second stage cooling rate/ (°C·s <sup>-1</sup> )	Transition temperature/ °C
0	0.5	0.5	–
2	2	0.43	617–616
3	2.3	0.44	616–615
3.5	2.6	0.44	615–614
4	3	0.43	614–613

After the IGs are added evenly into the liquid alloy, firstly there is an endothermic process. During the process, the cooling rate is faster. When the temperature of the IGs rises to solidus temperature, the liquid alloy is just near the liquidus temperature. As a result, when the IG size is set, the dosage is a critical process parameter. It is not only to ensure that the temperature of the liquid alloy is just near the liquidus temperature when the eutectic microstructure of the IG melts, but also to ensure that the eutectic microstructure is fully melted before the dumping.

#### 3.2 Effect of DT on slurry microstructure

Figure 4 shows the microstructures of the semi-solid slurries when the IG size is 10 mm, dosage is 3.5% and the DTs are 617, 615, 613 and 611 °C, respectively. According to the results, when the dumping temperature drops gradually from 617 to 611 °C, the

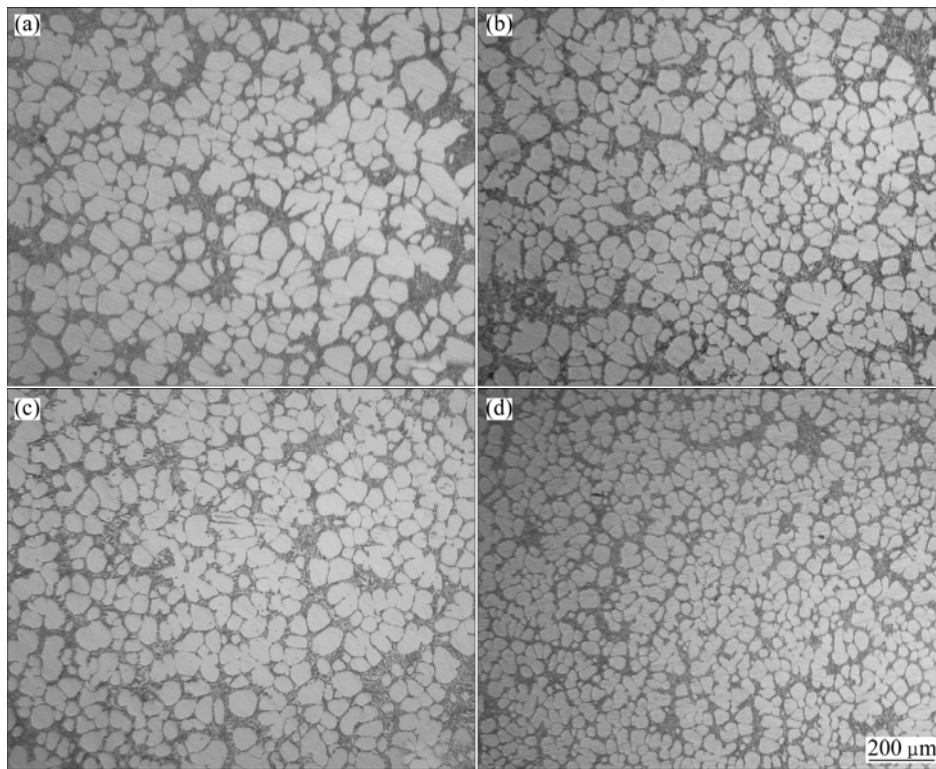


**Fig. 4** OM images showing slurry microstructures at different dumping temperatures: (a) 617 °C; (b) 615 °C; (c) 613 °C; (d) 611 °C

spherical or near-spherical primary  $\alpha(\text{Al})$  grains increase in number gradually, and the mean diameter decreases gradually from 75 to 40  $\mu\text{m}$ , and the shape factor increases gradually from 0.82 to 0.89. The slurry temperature and microstructure characteristics are listed in Table 2.

**Table 2** Effect of DT on slurry temperature and morphology

DT/°C	Slurry temperature/°C	Mean diameter/ $\mu\text{m}$	Shape factor
617	611	75	0.82
615	608	62	0.84
613	606	57	0.86
611	604	40	0.89

### 3.3 Effect of dosage on slurry microstructure

Figure 5(a) shows the slurry microstructure without IG, the primary  $\alpha(\text{Al})$  grains include rosettes and dendrites, and its morphology and diameter are difficult to measure. Figures 5(b), (c) and (d) show the slurry microstructures when the IG size is 10 mm, DT is 613 °C and the dosages are 2%, 3% and 4%, respectively. When the dosage is increased gradually from 2% to 4%, the spherical or near-spherical primary  $\alpha(\text{Al})$  grains increase in number gradually, the mean diameter decreases gradually from 82 to 45  $\mu\text{m}$  and the shape factor increases gradually from 0.78 to 0.88. The slurry

temperature and microstructure characteristics are listed in Table 3. When the dumping temperatures are the same, there is little effect of the dosage on the slurry temperature.

### 3.4 Effect of IG size on slurry microstructure

Figure 6 shows the slurry microstructures when the dosage is 3.5%, DT is 613 °C and IG sizes are 5 and 18 mm, respectively. When the IG size is 5 mm, the primary  $\alpha(\text{Al})$  grains are mainly near-spherical and rosettes, the mean diameter is 80  $\mu\text{m}$ , and the shape factor is 0.76. When the IG size is 18 mm, the primary  $\alpha(\text{Al})$  grains are mainly dendrites and rosettes, therefore, the morphology is poor, and the mean diameter and shape factor are difficult to measure. Comparing Fig. 6 with Fig. 4(c), it is seen that the IG with smaller or larger size is detrimental to improve the slurry microstructures.

## 4 Discussion

### 4.1 Formation mechanism of spherical primary $\alpha(\text{Al})$ grain

The primary  $\alpha(\text{Al})$  grains in the semi-solid slurry come mainly from two aspects. One is melted dendritic fragments of the IGs, it is why this preparation method is named introducing grain process (IGP); the other comes from the heterogeneous nucleation.

Because the melting point of eutectic microstructure

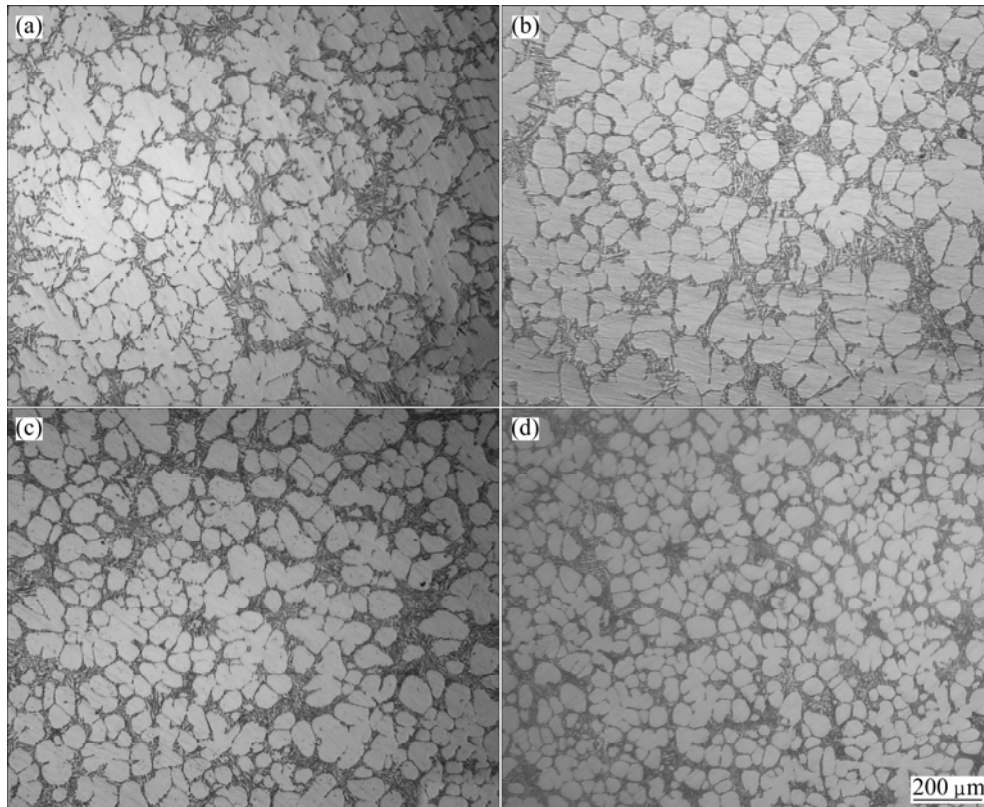


**Fig. 5** OM images showing Slurry microstructures with different dosages: (a) 0%; (b) 2%; (c) 3%; (d) 4%

**Table 3** Effects of IG dosage on slurry temperature and morphology at DT of 613 °C

Dosage/%	Slurry temperature/°C	Average diameter/μm	Shape factor
0	606	–	–
2	606	82	0.78
3	606	70	0.82
3.5	606	57	0.86
4	606	45	0.88

of the IG is lower, the eutectic microstructures of the edge area of the IG begin to melt. However, the melting point of the primary  $\alpha(\text{Al})$  dendrites is higher, and the original segregation at the roots of the dendritic arms leads to the constitutional undercooling, so the dendritic arms begin to fuse from the roots. During melting, a temperature undercooling area can be formed, as shown in Fig. 7. Because the IG is surrounded by the undercooling area, dendritic fragments of the primary  $\alpha(\text{Al})$  grains may not all melt into liquid phase, as a result, the remaining dendritic fragments become the direct source of the primary  $\alpha(\text{Al})$  grains. Many studies show that sufficient primary  $\alpha(\text{Al})$  nuclei in the semi-solid metal slurry is the necessary condition for the primary  $\alpha(\text{Al})$  nuclei to further spheroidize and prevent from growing too large [19,20]. From the experimental

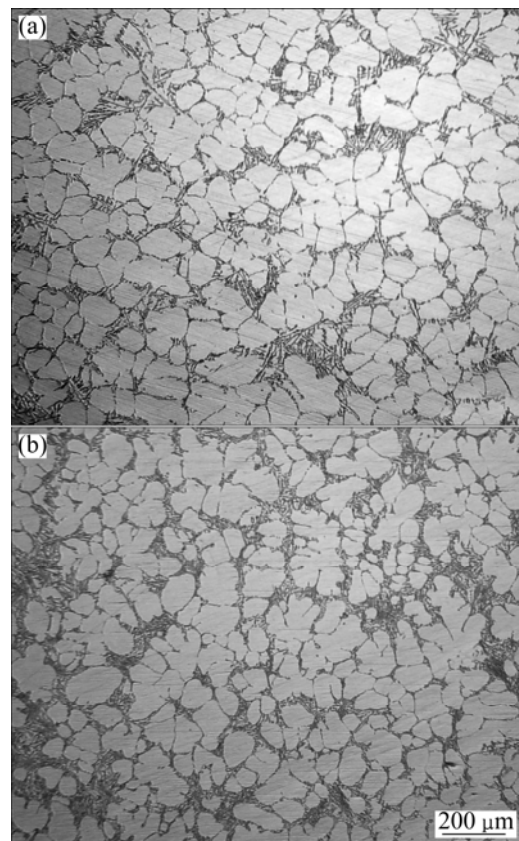


**Fig. 6** OM images showing slurry microstructures with different IG sizes: (a) 5 mm; (b) 18 mm

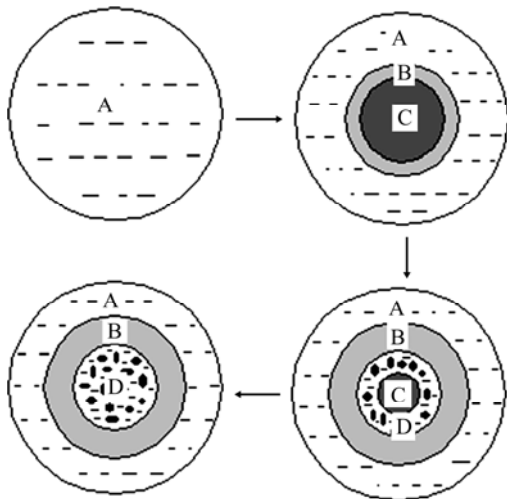


**Fig. 7** Schematic diagrams of IG melting and formation of undercooling area: (A—Liquid alloy; B—Undercooling area; C—IG; D—Melting dendritic fragments)

results at DT of 617 °C, the alloy temperature is slightly higher than the liquidus temperature, but most of the dendritic fragments can be saved, this is because there exist a large number of undercooling areas.

The IG not only offers a number of primary  $\alpha(\text{Al})$  grains but also many undercooling areas, where heterogeneous nucleation is favorable, and the mechanism of the heterogeneous nucleation agrees well with that of liquidus casting process [21]. The lower the DT is, the more the number of the primary  $\alpha(\text{Al})$  grains is by heterogeneous nucleation, and the better the slurry microstructure is. The dumping aims to not only the entire alloy temperature uniformity and the primary  $\alpha(\text{Al})$  grains spread evenly throughout the alloy melt, but also the ripening of the primary  $\alpha(\text{Al})$  grains because of the temperature fluctuation by mixing the undercooling areas and the surrounding liquid alloy.

#### 4.2 Morphology controlling of primary $\alpha(\text{Al})$ grain

When the IG is added to the liquid alloy, whether the alloy melt can become sound semi-solid slurry is theoretically decided by the following two formulas:

$$Q_R = M_L(C_T T - 615C_L) \quad (1)$$

$$Q_A = M_S(577C_S - C_0 T_1) \quad (2)$$

where  $Q_R$  is the releasing heat of liquid alloy dropping to liquidus temperature;  $M_L$  is the mass of liquid alloy;  $C_T$  is the specific heat capacity of liquid alloy at temperature  $T$ ;  $T$  is the temperature of liquid alloy;  $C_L$  is the specific heat capacity of liquid alloy at liquidus temperature;  $Q_A$  is the absorption heat of the IG rising to solidus temperature;  $M_S$  is the mass of the IG;  $C_S$  is the specific heat capacity of the IG in solidus temperature;  $C_0$  is the specific heat capacity of the IG at room temperature;  $T_1$

is the temperature of the IG.

During the actual preparation, the heating rate of IG ( $R_h$ ) and cooling rate of liquid alloy ( $R_c$ ) must be also considered. During the temperature of the liquid alloy dropping to liquidus temperature, as long as the heat of liquid alloy releasing to the surrounding environment is much less than that of the IG absorbing, the heat loss can be ignored. Then, the morphology of the primary  $\alpha(\text{Al})$  grains in semi-solid slurry can be determined qualitatively based on the following conditions.

1) When  $Q_R = Q_A$ , if  $R_h = R_c$ , that is, when the temperature of the IG rises to the solidus temperature, the liquid alloy just drops to the liquidus temperature. At this time, the liquid alloy solidification latent heat is enough to melt the eutectic microstructure of the IG, as long as the DT is suitable, sound semi-solid slurry can be produced; if  $R_h > R_c$ , this indicates that the IG size is too small, as a result, the IG all melts into liquid phase; if  $R_h < R_c$ , this indicates that the IG size is too large, as a result, the dendritic microstructure of the IG appears in the semi-solid slurry, as shown in Fig. 6(b).

2) When  $Q_R > Q_A$ , this indicates that the dosage is too little, as a result, the IG all melts into liquid phase, the primary  $\alpha(\text{Al})$  grains come mainly from heterogeneous nucleation, and the microstructure of the semi-solid slurry is poor, as shown in Fig. 5(b); when  $Q_R < Q_A$ , this indicates that the dosage is too much, as a result, genetic effect of dendrites in the IG on the semi-solid slurry is more obvious.

## 5 Conclusions

1) During the preparation of the semi-solid A356 Al-alloy slurry by IGP, when the IG size is 10 mm, the dosage is 3.5% and the DT is 611–617 °C, the mean diameter of the primary  $\alpha(\text{Al})$  grains in the slurry can reach 40–75  $\mu\text{m}$ , and the shape factor can reach 0.82–0.89. With decreasing DT, the microstructure of the primary  $\alpha(\text{Al})$  grains is better.

2) When the IG size is 10 mm, the DT is 613 °C, the dosage is 2%–4%, the mean diameter of the primary  $\alpha(\text{Al})$  grains can reach 45–82  $\mu\text{m}$ , and the shape factor can reach 0.78–0.88. With the dosage increasing properly, the microstructure of the primary  $\alpha(\text{Al})$  grains is better.

3) When  $Q_R = Q_A$  and  $R_h = R_c$ , as long as the DT is suitable, sound semi-solid slurry can be produced; when  $Q_R > Q_A$  or  $Q_R < Q_A$ , it is difficult to produce sound semi-solid slurry.

4) The dendritic fragments from IG become the direct source of the primary  $\alpha(\text{Al})$  grains in the semi-solid slurry. The temperature undercooling area from the IG melting provides favorable conditions for heterogeneous nucleation.

## References

- [1] JI S, FAN Z, BEVIS M J. Semi-solid processing of engineering alloys by a twin-screw rheomolding process [J]. *Mater Sci and Eng A*, 2001, 299: 210–217.
- [2] MAO Wei-min, ZHEN Zi-sheng, CHEN Hong-tao, ZHONG Xue-you. Microstructural formation of semi-solid AZ91D alloy stirred by electromagnetic field [J]. *Journal of University of Science and Technology Beijing: Mineral Metallurgy Materials (Eng Ed)*, 2005, 12(4): 329–334.
- [3] TANG Meng-ou, XU Jun, ZHANG Zhi-feng, BAI Yue-long. New method of direct casting of Al–6Si–3Cu–Mg semisolid billet by annulus electromagnetic stirring [J]. *Transactions of Nonferrous Metals Society of China*, 2010, 20(s): s1591–s1596.
- [4] KAUFMANN H, MUNDL A, UGGOWITZER P J, POTZINGER R, ISHIBASHI N. An update on the new rheocasting-development work for Al- and Mg-alloys [J]. *Die Casting Engineer*, 2002, 46(4): 16–19.
- [5] GAO Ming, WANG Ping, LU Gui-min, CUI Jian-zhong. Microstructures of an AlSi<sub>7</sub>Mg alloy by near-liquidus casting [J]. *Rare Metals*, 2007, 26(3): 226–229.
- [6] TOSHIO H, KAPRANOS P. Simple rheocasting processes [J]. *Journal of Materials Processing Technology*, 2002, 130–131: 594–598.
- [7] YURKO J, BONI R. SSR™ semi-solid rheocasting [J]. *Metallurgia Italiana*, 2006, 98(3): 35–41. (in Italian)
- [8] CHEN Zheng-zhou, MAO Wei-min, WU Zong-chuang. Mechanical properties and microstructures of Al-alloy tensile samples produced by serpentine channel pouring rheo-diecasting process [J]. *Transactions of Nonferrous Metals Society of China*, 2011, 21(7): 1473–1479.
- [9] LI Hui, LI Ping, XUE Ke-min. Study on refining of semisolid Al-alloy by Ti–B [J]. *Foundry Technology*, 2005, 26(12): 1106–1108. (in Chinese)
- [10] LIU Zheng, HU Yong-mei. Effect of yttrium on the microstructure of a semi-solid A356 Al alloy [J]. *Rare Metals*, 2008, 27(5): 536–540.
- [11] ZHAO Zu-de, CHEN Qiang, KANG Feng, SHU Da-yu. Microstructural evolution and tensile mechanical properties of thixoformed AZ91D magnesium alloy with the addition of yttrium [J]. *Journal of Alloys and Compounds*, 2009, 482(1/2): 455–467.
- [12] OHMI T, MINEGUCHI K, KUDOH M, ITOH Y, MATSUURA K. Control of primary silicon crystal size of semi-solid hypereutectic Al–Si alloy by slurry-melt mixing process [J]. *Journal of the Japan Institute of Metals*, 1994, 58(11): 1311–1317. (in Japanese)
- [13] ZENG Yi-dan, SHI Li-kai, ZHANG Zhi-feng, LIANG Bo, XU Jun. Effects of processing parameters on the microstructure of semi-solid slurry prepared by melt spreading and mixing method [J]. *Special Casting and Nonferrous Alloys*, 2008, 28(6): 435–438. (in Chinese)
- [14] TEBIB M, MORIN J B, AJERSCH F, GRANTCHEN X. Semi-solid processing of hypereutectic A390 alloys using novel rheoforming process [J]. *Transactions of Nonferrous Metals Society of China*, 2010, 20(s): s1743–s1748.
- [15] CHEN Zhen-hua, YAN Hong-ge, CHEN Gang, ZHANG Fu-quan, HU Zhong-xun, FU Jie-xing. Mixed solid liquid casting processing of Al–8.7Fe–1.6V–1.3Si elevated temperature alloy [J]. *The Chinese Journal of Nonferrous Metals*, 2002, 12(3): 422–425. (in Chinese)
- [16] REN Zheng, ZHANG Xing-guo, FANG Can-feng, HAO Hai. Effect of electromagnetic suspension casting on grain refinement for wrought magnesium alloy [J]. *Chinese Journal of Materials Research*, 2007, 21(5): 491–495. (in Chinese)
- [17] LI Yuan-dong, YANG Jian, MA Ying, QU Jun-feng, ZHANG Peng. Effect of pouring temperature on AM60 Mg alloy semi-solid slurry prepared by self-inoculation method (I) [J]. *The Chinese Journal of Nonferrous Metals*, 2010, 20(6): 1046–1052. (in Chinese)
- [18] LI Yuan-dong, YANG Jian, MA Ying, QU Jun-feng, ZHANG Peng. Effect of inoculant parameters on AM60 Mg alloy semisolid slurry prepared by self-inoculation method (II) [J]. *The Chinese Journal of Nonferrous Metals*, 2010, 20(11): 2178–2186. (in Chinese)
- [19] ZHAO Jian-xin, ZHU Ming-fang, KIM Jie-min, HONG Chun-pyo. Evolution of globular and dendritic structures in solidification of Al–Si alloys [J]. *Physical Testing and Chemical Analysis A: Physical Testing*, 2004, 40(9): 433–438. (in Chinese)
- [20] GUO Hong-min, YANG Xiang-jie. Formation mechanism of spherical particles in undercooled melt [J]. *The Chinese Journal of Nonferrous Metals*, 2008, 18(4): 651–659. (in Chinese)
- [21] DONG Jie, LU Gui-min, REN Qi-feng, CUI Jian-zhong. Discussion on the formation mechanism of nondendritic semisolid microstructures during liquidus casting [J]. *Acta Metallurgica Sinica*, 2002, 38(2): 203–207. (in Chinese).

## 引晶法制备半固态 A356 铝合金浆料

陈正周

汇丽机电有限公司, 慈溪 315333

**摘要:** 开发一种半固态金属浆料制备技术, 即引晶法, 研究工艺参数对半固态 A356 铝合金浆料组织的影响, 讨论球状初生  $\alpha(\text{Al})$  晶粒的形成机制和形貌控制。结果表明: 当制备浆料为 4 kg、引晶尺寸为 10 mm、加入量为 3.5%、倾倒入温度为 611–617 °C 时, 半固态浆料中初生  $\alpha(\text{Al})$  晶粒的平均直径可达 40–75  $\mu\text{m}$ , 形状因子可达 0.82–0.89。当引晶尺寸为 10 mm、倾倒入温度为 613 °C、加入量为 2%–4% 时, 初生  $\alpha(\text{Al})$  晶粒的平均直径可达 45–82  $\mu\text{m}$ , 形状因子可达 0.78–0.88。倾倒入温度的降低或者引晶加入量的适当增加, 可以改善初生  $\alpha(\text{Al})$  晶粒的组织。当  $Q_R = Q_A$ 、 $R_h = R_c$  时, 只要倾倒入温度适宜就可以制备优质半固态浆料。引晶熔化时产生的枝晶碎块是半固态浆料中初生  $\alpha(\text{Al})$  晶粒的直接来源, 形成的温度过冷区也有利于异质形核。

**关键词:** A356 铝合金; 半固态; 引晶; 初生  $\alpha(\text{Al})$

(Edited by FANG Jing-hua)